Tilt of Pancake Vortex Stacks in Layered Superconductors in the Crossing Lattice Regime

A. N. Grigorenko,[1] S. J. Bending,[2] I. V. Grigorieva,[1] A. E. Koshelev,[3] T. Tamegai,[4] and S. Ooi[4]

[1]*Department of Physics and Astronomy, University of Manchester, Manchester M13 9PL, United Kingdom*
[2]*Department of Physics, University of Bath, Claverton Down, Bath BA2 7AY, United Kingdom*
[3]*Materials Science Division, Argonne National Laboratory, Argonne, Illinois 60439, USA*
[4]*Department of Applied Physics, University of Tokyo, Hongo, Bunkyo-ku, Tokyo 113-8656, Japan*
(Received 24 September 2004; published 14 February 2005)

We study crossing vortices in strongly anisotropic $Bi_2Sr_2CaCu_2O_{8+\delta}$ single crystals. Using scanning Hall probe microscopy and Bitter decoration techniques, we find an asymmetry of magnetic field profiles produced by pancake vortices (PVs), which are interacting with Josephson vortices (JVs), near the surface of the crystal. We attribute the observed asymmetry to a substantial tilt (14–18 degrees) of PV stacks, which is produced by the torque due to the surface currents and JVs. We calculate the tilt angle and obtain agreement with experimental data when the irreversible in-plane magnetization is included. A further refinement to the model is considered which accounts for a reduction in the PV stack line tension near the sample surface.

Among the most exciting vortex states in layered superconductors [1–15] are the crossing lattices where a tilted magnetic field generates two relatively independent lattices [4–7]: a greatly stretched rhombic lattice of Josephson vortices (JVs) (running parallel to the *a-b* plane) and the perpendicular Abrikosov lattice of pancake vortex (PV) stacks (normal to the CuO_2 layers). Crossing vortices in layered superconductors experience an attraction [7,9]. As a result, some PV stacks become "trapped" by JVs and make vortex chains along JV lines, effectively "decorating" them [10].

Crossing vortices are a topic of major current interest. The trapped PV stacks (chain vortices) allow one to study the Josephson vortex behavior which is difficult to elucidate by other means [10–12]. Furthermore, the PV-JV interactions promise a variety of interesting applications including vortex pumps, lenses, and a distant prospect of vortex logic [10–13]. Recently, a quantitative theory of crossing vortices has been elaborated [7] and found strong experimental support from direct observations by scanning Hall probe [10,14] and Lorentz [12] microscopies, magneto-optics [11], and indirect measurements of vortex melting [15].

In this Letter, we refine the accepted picture of crossing vortices [7]. We show that the crossing PV and JV lattices are not exactly perpendicular. Instead, PV stacks are tilted with respect to the crystalline *c* axis under the action of the torque generated by surface and JV currents. Using two different experimental techniques of scanning Hall probe microscopy (SHPM) and Bitter decorations, we show an asymmetry of magnetic field profiles produced by PVs, which we attribute to a PV stack tilt, and estimate the tilt angle from this asymmetry. We relate the PV tilt to the in-plane magnetization and describe changes in the PV line structure intersected by a JV stack near the sample surface.

The experiments were performed on freshly cleaved $Bi_2Sr_2CaCu_2O_{8+\delta}$ (Bi-2212) single crystals with anisotro-pies γ in the range from 300 to 600. The anisotropy parameter γ was determined from the chain separation in the crossing-lattice state of vortex matter as explained in [7,10]. The crystal sizes were in the mm range, the thickness *d* was about 10–100 μm, and the *c* axis was perpendicular to the sample surface. SHPM and Bitter decoration techniques have been used to study the vortex matter. SHPM produces a map of magnetic induction perpendicular to the sample surface at a distance of 400–600 nm above the surface [16]. In contrast, the Bitter decoration technique is sensitive to the magnetic field gradients at the sample surface [17].

First we demonstrate that PV stacks in crossing states produce an asymmetric distribution of magnetic induction above the sample surface. Figure 1(a) shows the Bitter pattern of the sample cooled in the field of $H = 20$ Oe applied at an angle of 70° with respect to the *c* axis of the crystal. Bitter decoration was performed with 15–20 nm Fe particles thermally evaporated onto the superconductor (the temperature of the sample at the moment of decoration was about 10 K). One can see the regions of the Abrikosov lattice separated by vortex chains residing on JV stacks indicated by black arrows. The chain separation c_y yields the sample anisotropy parameter γ within the anisotropic London theory as $\gamma = 2c_y^2 B_{ab}/(\sqrt{3}\Phi_0) \approx 300$, where B_{ab} is the in-plane component of magnetic induction and Φ_0 is the flux quantum [7,18].

The insets of Fig. 1(b) display averaged Bitter images of PVs inside and outside the JV stacks. The surface density of deposited Bitter particles reflects the local value of magnetic induction, *B*, and is expected to be proportional to B^2. The average Bitter patterns were obtained by cutting out individual Bitter images of 32 different vortices inside/outside the vortex chains and then taking a linear average. (The center of "mass" of an individual vortex image was used as a guide to vortex positioning.) We note two important features of these averaged patterns. The Bitter
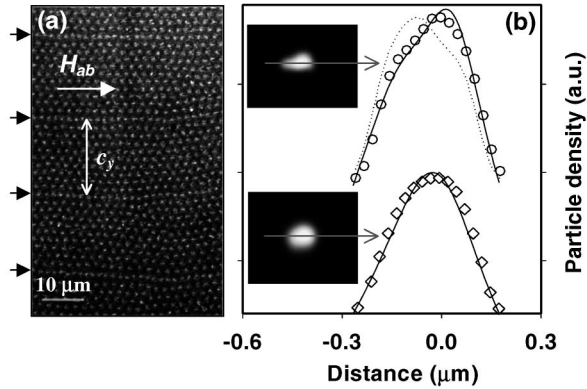
FIG. 1. Bitter decoration. (a) A Bitter image of vortices in a Bi-2212 single crystal cooled in a field of $H = 20$ Oe applied at an angle of $70°$. The white arrow indicates the ab-plane field direction; the black arrows mark the positions of PV chains. (b) The top/bottom insets show the averaged Bitter image of a PV inside/outside a JV stack. The graph plots the line scans (circles and diamonds) of averaged images along the line indicated by gray arrows. The dotted line is the mirrored line scan of the Bitter image of a PV inside a JV stack. The top/bottom solid lines represent the calculated B_z^2 (see text) for a tilted PV stack inside JV cores and a straight PV stack outside JVs, respectively, for the conditions of $c_y = 18$ μm, $\lambda = 200$ nm, and the PV line tilt angle of $70°$.

pattern of PVs inside the chain has a distinct elongated shape with an aspect ratio of about 2, while the average PV shape outside the chain is circular to an accuracy of 10%. This elongated shape of the average Bitter image of trapped PVs is indeed expected due to PV displacements induced by JV currents, as predicted by theory [7] and observed in SHPM experiments [14]. In addition, the average shape of decorated PVs and, hence, the magnetic field distribution at the surface of the sample is clearly asymmetric: Compare the line scan (circles) with the mirrored line scan (the dotted line) in Fig. 1(b).

The asymmetry of the magnetic induction produced by PV stacks was also observed in SHPM measurements. Figures 2(a) and 2(b) show maps of magnetic induction (SHPM images) measured with the scanning Hall probe retracted about 500 nm from the surface of the sample. SHPM experiments were performed on a different crystal with anisotropy $\gamma = 640$. The sample had been zero-field cooled to the target temperature after which an ab field and a c field were applied. The figure shows two examples ($T = 85$ K and $T = 83$ K) where the ab field has two different magnitudes (35 Oe, 20 Oe) and two distinct directions with respect to the crystallographic a axis. The SHPM image [2(a)] contains an isolated PV stack trapped by a JV stack (the JV stack is indicated by black arrows and seen as a faint white line of "sublimed" PVs described in [10] which are supposed to be either tilted/kinked or melted), and 2(b) depicts a row of PV lines trapped by JVs also indicated by black arrows. The PV stack in Fig. 2(a) has, again, an elongated shape due to PV displacements induced by JV currents. Furthermore, similar to
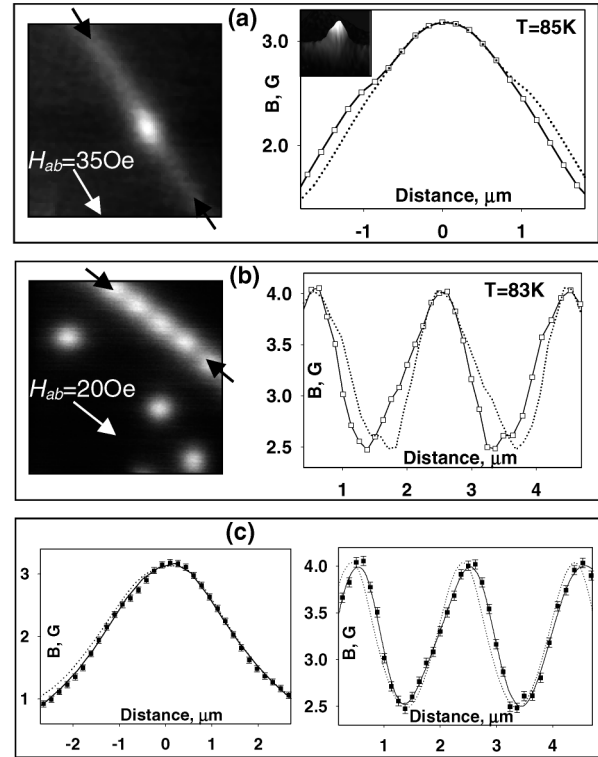

FIG. 2. (a) Left: SHPM image of the zero-field-cooled sample subject to fields of $H_{ab} = 35$ Oe and $H_c = 2$ Oe at $T = 85$ K, the image size 21×21 μm^2, gray scale (GS) = 2G. Right: magnetic induction along the JV line (black arrows), squares and the solid line, and the mirrored magnetic induction, the dotted line. The inset shows a zoomed 3D SHPM image of the trapped PV. (b) The same for the zero-field-cooled sample subject to $H_{ab} = 30$ Oe, $H_c = 2$ Oe and then $H_{ab} = 20$ Oe, $H_c = 0$ Oe at $T = 83$ K, image size 14×14 μm^2 (GS = 5.6). (c) Fits to the measured magnetic line scans of (a) and (b) using the theoretical model described in the text for a tilted PV line (solid line) and an untilted PV line (dotted line).

Bitter decorations, SHPM reveals that the map of magnetic induction above a PV stack residing inside the JVs is not symmetric, as is clear from comparison of the line scans of Figs. 2(a) and 2(b) (solid lines) with the mirrored line scans (dotted lines).

The observed asymmetry of magnetic field profiles generated by the PVs has a natural explanation in the tilt of PV lines induced by surface and JV currents, as we show below. Indeed, JV and surface currents exert Lorentz forces F_{JV} and F_s on a PV stack crossing a JV stack which displace PVs with respect to an average PV line position [7] as illustrated in Fig. 3(a). The total force produced by the JV and surface currents on a PV line is zero; however, the net torque is not. The torque tilts a PV line [solid lines in Figs. 3(a)–3(c)] crossed by a JV stack [horizontal dotted segments in Figs. 3(b) and 3(c)] with respect to the c axis (dashed lines). The *homogeneously tilted* PV line structure describes well the asymmetry of magnetic fields observed in SHPM and Bitter decoration measurements. The magnetic induction at a height h above an isolated PV stack is
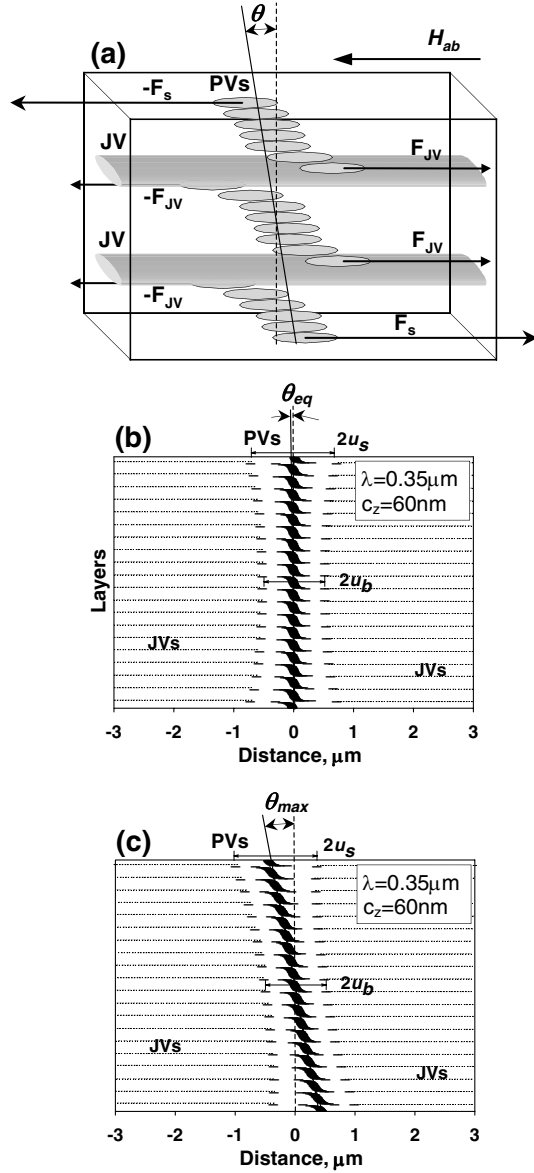
FIG. 3. Structure of a PV stack intersected by a JV stack. The PV line is tilted at an angle θ with respect to the c axis (vertical dashed line). (a) Schematic view. (b) Equilibrium structure. Dashed symbols represent PVs; horizontal dotted lines show JVs. (c) PV structure for states with maximum magnetization.

given by [19]

$$B_z(x,h) = \frac{s\Phi_0}{2\pi\lambda^2} \sum_{n=0}^{d/s} \int_0^\infty \frac{\exp(-\sqrt{t^2 + \lambda^{-2}}ns - th)}{\sqrt{t^2 - \lambda^{-2}} + t}$$
$$\times J_0[t(x - u_n)]t\,dt, \qquad (1)$$

where u_n are pancake displacements [7] and $J_0(x)$ is the Bessel function. Inserting the (homogeneous) tilt angle of a PV line as a fitting parameter, we get an excellent fit to the measured asymmetric magnetic induction profiles, virtually without free adjustable parameters [see the solid lines in Fig. 2(c)]. The PV wandering length r_w (which enters into the pancake displacements u_n, see [7]) was the only

parameter adjusted near the sample surface, and care was taken to include the effects of surface barriers on the depth of the first JV beneath the sample surface [20]. For comparison, the dotted lines of Fig. 2(c) show the calculated magnetic inductions for the structured *untilted* PV lines, which fail to describe the asymmetry of the measured magnetic induction. The tilt angle extracted from the best fit is 18° for Fig. 2(a) and 14° for Fig. 2(b). The model (1) with tilted PV lines also provides a good description of the average vortex patterns obtained from Bitter decorations. Figure 1(b) shows a fit of the calculated B_z^2 (proportional to the density of Fe particles) to the measured profiles of the particle distributions (the estimated tilt angle is 17°).

The magnitudes of extracted tilt angles are in reasonable agreement with theory. Within the anisotropic London theory, the torque per unit length experienced by a PV stack equals $t = \frac{1}{d}\int_0^d zF(z)dz = \frac{\Phi_0}{cd}\int_0^d zj(z)dz$, where $j(z)$ is the current at the position of a PV line and c is the speed of light. The torque t is compensated by the restoring torque arising from an energy change of a tilted PV stack [2], $\Delta E(\theta) = \varepsilon_0 \ln[(1 + \cos\theta)/(2\cos\theta)]$. This gives the tilt angle of a PV line intersected by a JV stack in the bulk of the superconductor,

$$\theta \approx \frac{2t}{\varepsilon_0}, \qquad (2)$$

where $\varepsilon_0 = [\Phi_0/(4\pi\lambda)]^2$, $\lambda = \lambda_{ab}$ is the ab-plane penetration depth. For our experimental case of a JV lattice with overlapping JV currents [21] [$s < c_z < \lambda$ where $c_z = \sqrt{\sqrt{3}\Phi_0/(2\gamma B_{ab})}$ is the distance between JVs in a stack], the torque t can be related to the in-plane magnetization M_{ab}. Indeed, the local in-plane current can be split into the lattice averaged and oscillating contributions $j_y(y,z) = \langle j_y(z)\rangle + \delta j_y(y,z)$ (for an ab field applied along the x direction). The lattice averaged current determines the in-plane magnetization $M_{ab} = \frac{1}{cd}\int_0^d z\langle j_y(z)\rangle dz$. Comparing the expressions for magnetization and the torque, we get $t \approx \Phi_0 M_{ab}$. [The difference appears due to the lattice oscillating currents $\delta j_y(0,z)$ and will be discussed elsewhere. It is small when $c_z < \lambda$.] We conclude, therefore, that all PV stacks in the crossing states of layered superconductors should be tilted with respect to the c axis by an angle

$$\theta = \frac{2\Phi_0 M_{ab}}{\varepsilon_0}. \qquad (3)$$

Thus, the Abrikosov and Josephson lattices of crossing states are not exactly perpendicular. The skew angle between crossing lattices is proportional to the in-plane magnetization. The irreversible in-plane magnetization depends upon the history of the prepared state; therefore, the tilt angle is *history dependent*. The equilibrium magnetization is $M_{eq} = -\frac{\Phi_0}{2(4\pi\lambda)^2\gamma}\ln(2.77B_{cr}/B_{ab})$ [22] and the equilibrium tilt angle is $\theta_{eq} \approx \frac{1}{\gamma}\ln(B_{cr}/B_{ab})$, where $B_{cr} = \Phi_0/(\pi\gamma s^2)$ is the crossover field. The equilibrium tilt angle

is small (for our samples it is of the order of 1° which is much smaller than the tilt angles estimated from the asymmetry of magnetic field profiles). To evaluate the tilt angle for nonequilibrium states, we use the fact that in homogeneous Bi-2212 crystals the penetration field is determined by surface barriers [23] which yields the maximum value of magnetization as $M_{\max} = -\frac{\varepsilon_0}{2\pi B_{ab}(\gamma s)^2}$ [24]. This maximum magnetization corresponds to the maximum possible tilt angle in the bulk for any nonequilibrium state:

$$\theta_{\max} \approx \frac{\Phi_0}{\pi B_{ab}(\gamma s)^2}. \tag{4}$$

The experimental tilt angle is defined by the actual in-plane magnetization and should be smaller than this maximum tilt (4). Expression (4) gives the right order of magnitude for the tilt angles discussed above ($\theta_{\max} \approx 60°$ for the conditions of the Bitter decorations shown in Fig. 1 and $\theta_{\max} \approx 10°$ for the conditions of the SHPM measurements in Fig. 2).

The described theory calculates the average PV tilt in the bulk of the superconductor. To allow a quantitative comparison with experiments it should be elaborated further to take into account additional changes of PV and JV properties near the surface of a superconductor [17,25–27]. One change is connected with the nonlocality of the PV line tension. In the discussed case of large γ, the line tension is produced by an attraction of PVs of different layers and is smaller near the surface (compared to the bulk value) because of the absence of PVs above the sample. A simple estimate, that neglects thermal fluctuations and a change of PV currents near the surface of a superconductor, yields the reduction factor in line tension as $[1 - \exp(-z/\lambda)/2]$, where z is the distance measured from the surface. We illustrate the change in structuring of a PV stack intersected by JVs near the surface in Figs. 3(b) and 3(c), where the PV stack structure is calculated in the limit of electromagnetic coupling for a 1.2 μm thick film. Figure 3(b) shows the equilibrium state and 3(c) the state with maximum in-plane magnetization calculated for $\lambda = 0.35$ μm, $c_z = 40s$, and $\gamma = 640$. These calculations result in $\theta_{\mathrm{eq}} \approx 0.5°$ and $\theta_{\max} \approx 40°$ which agree with the analysis above. Figures 3(b) and 3(c) show the increase of PV displacements near the sample surface arising due to the decrease of the PV line tension (compare the bulk values of u_b with the surface values u_s). As a result, the crossing energy [7] near the sample surface is twice as big as the bulk values.

The discussed structure of a PV line crossed by a JV stack has a pronounced effect on vortex interactions [28] in crossing-lattice states of layered superconductors as well as their magnetization. For example, the tilt produces a dipole moment for all PV lines (even in the Abrikosov regions in between JV stacks), which generates an attraction between PV stacks [29]. The most dramatic changes are expected for trapped PVs at high temperatures and relatively large H_c fields, where $\lambda(T) \gtrsim \gamma s$ and the equi-

librium distance between PV lines along a JV stack $a \sim 2\lambda \ln(\lambda/u)$ [29] becomes comparable with the PV displacements $u \sim \lambda^2/(\gamma s)$ [7]. This will be addressed elsewhere [30].

---

[1] K. B. Efetov, Sov. Phys. JETP **49**, 905 (1979).
[2] J. R. Clem, Phys. Rev. B **43**, 7837 (1991); J. R. Clem and M. W. Coffey, Phys. Rev. B **42**, 6209 (1990); J. R. Clem, Supercond. Sci. Technol. **11**, 909 (1998).
[3] L. N. Bulaevskii, M. Ledvij, and V. G. Kogan, Phys. Rev. B **46**, 366 (1992).
[4] C. A. Bolle *et al.*, Phys. Rev. Lett. **66**, 112 (1991).
[5] I. V. Grigorieva, J. W. Steeds, G. Balakrishnan, and D. M. Paul, Phys. Rev. B **51**, 3765 (1995).
[6] D. A. Huse, Phys. Rev. B **46**, 8621 (1992).
[7] A. E. Koshelev, Phys. Rev. Lett. **83**, 187 (1999).
[8] A. Sudbo and E. H. Brandt, Phys. Rev. Lett. **67**, 3176 (1991).
[9] L. N. Bulaevskii *et al.*, Phys. Rev. B **53**, 6634 (1996).
[10] A. N. Grigorenko, S. J. Bending, T. Tamegai, S. Ooi, and M. Henini, Nature (London) **414**, 728 (2001).
[11] M. Yasugaki *et al.*, Phys. Rev. B **65**, 212502 (2002); V. K. Vlasko-Vlasov *et al.*, Phys. Rev. B **66**, 014523 (2002); M. Tokunaga, M. Kobayashi, Y. Tokunaga, and T. Tamegai, Phys. Rev. B **66**, 060507 (2002).
[12] A. Tonomura *et al.*, Phys. Rev. Lett. **88**, 237001 (2002).
[13] S. Savel'ev and F. Nori, Nat. Mater. **1**, 179 (2002).
[14] A. N. Grigorenko *et al.*, Phys. Rev. Lett. **89**, 217003 (2002).
[15] S. Ooi *et al.*, Phys. Rev. Lett. **82**, 4308 (1999); J. Mirkovic, S. E. Savel'ev, E. Sugahara, and K. Kadowaki, Phys. Rev. Lett. **86**, 886 (2001).
[16] A. Oral, S. J. Bending, and M. Henini, Appl. Phys. Lett. **69**, 1324 (1996).
[17] U. Essmann and H. Trauble, Phys. Lett. **24A**, 526 (1967).
[18] L. J. Campbell, M. M. Doria, and V. G. Kogan, Phys. Rev. B **38**, 2439 (1988).
[19] J. R. Clem, Physica (Amsterdam) **235C–240C**, 2607 (1994); (unpublished).
[20] A. E. Koshelev, Physica C (Amsterdam) **223**, 276 (1994); (unpublished).
[21] In the case of $c_z > \lambda$, the tilt angle is given by $\theta = 4\pi\lambda/(\gamma c_z) - \Phi_0 H_{ab}/(2\pi\varepsilon_0)$.
[22] V. G. Kogan, M. M. Fang, and S. Mitra, Phys. Rev. B **38**, 11958 (1988).
[23] H. Enriques *et al.*, Phys. Rev. B **63**, 144525 (2001).
[24] The calculation of the maximum magnetization will be reported elsewhere.
[25] E. H. Brandt, R. G. Mints, and I. B. Shapiro, Phys. Rev. Lett. **76**, 827 (1996).
[26] V. Pudikov, Physica C (Amsterdam) **212**, 155 (1993).
[27] H. Fangohr, A. E. Koshelev, and M. J. W. Dodgson, Phys. Rev. B **67**, 174508 (2003).
[28] M. J. W. Dodgson, Phys. Rev. B **66**, 014509 (2002).
[29] A. Buzdin and I. Baladie, Phys. Rev. Lett. **88**, 147002 (2002).
[30] A. E. Koshelev (to be published).